J Solid State Electrochem (2005) 9: 347–353
DOI 10.1007/s10008-004-0625-7

ORIGINAL PAPER

G. G. Láng · M. Seo · K. E. Heusler

Simultaneous oscillations of surface energy, superficial mass and electrode potential in the course of galvanostatic oxidation of formic acid

Received: 10 September 2004 / Revised: 28 October 2004 / Accepted: 28 October 2004 / Published online: 6 April 2005

Abstract Simultaneous oscillations of electrode potential, surface mass and specific surface energy have been detected in the course of galvanostatic oxidation of formic acid on platinum by using a Koesters laser interferometer combined with an electrochemical quartz crystal microbalance. Changes of surface energy data measured with the electrochemical Koesters laser interferometer and with the electrochemical bending beam technique are shown to be equivalent. Problems related to the interpretation of the measured data are discussed.

Keywords Surface energy · Surface stress · Superficial mass · Formic acid · Koesters laser interferometer · Bending beam method

Introduction

Potential or current oscillations during the galvanostatic or potentiostatic oxidation of organic compounds at noble metal electrodes have been known to exist for a long time, and have been the topic of many experimental and theoretical studies [1–6]; however, periodical changes of the electrode potential under galvanostatic or open-circuit conditions, or periodical fluctuations of current under potentiostatic conditions have been observed also in a number of other electrochemical systems [7–11].

Periodic oscillations of the electrode potential during the potentiostatic oxidation of formaldehyde and formic acid at platinum in acidic solutions were observed frequently [4–6, 12–16]. In particular, the oxidation of formic acid was extensively studied since the early 1960s, because it is an important reaction in the methanol fuel cell and is also a good model system to investigate the mechanism of electrooxidation of small organic molecules [16].

The majority of oscillation mechanisms proposed so far involve the formation and decomposition of an inhibiting surface layer, which may consist of chemisorbed species or insoluble salts [17–20]. In the model of Albahadily and Schell [17], six or seven variables with nine or ten reaction steps, an autocatalytic step, and the number of vacant adsorption sites are involved. The model proposed by Strasser et al. [18], which uses four variables including the diffusion of formic acid from the bulk solution to the interface, describes well the various potentiostatic oscillations observed. The model with only three variables proposed in [19] was analyzed from the point of view of nonlinear dynamics in [20]. It assumes a potential-dependent adsorption and desorption reaction and the reaction of chemisorbed H_2O and CO. This model also accounts well for the observed galvanostatic potential oscillations.

Some efforts have been made to follow the changes of the surface composition by radiotracer [21], ellipsometric [22], and probe beam deflection (PBD) methods [23], and the changes of the adsorbed mass using the electrochemical quartz crystal microbalance [24]. However, there is little direct information concerning the energetics of the surface during the oscillation cycles. Results of experiments concerning the simultaneous changes of the electrode potential and of the generalized surface parameter γ^s with contributions from both the

Dedicated to Professor György Horányi on the occasion of his 70th birthday

G. G. Láng (✉)
Department of Physical Chemistry,
Eötvös Loránd University,
Budapest, Pázmány Péter sétány 1/A,
1117, Hungary
E-mail: langgyg@para.chem.elte.hu
Tel.: +36-1-2090555
Fax: +36-1-2090602

M. Seo
Graduate School of Engineering,
Hokkaido University,
Sapporo, Japan

K. E. Heusler
Technische Universität Clausthal,
Clausthal, Germany

superficial energy and the surface stress [25] were reported only for galvanostatic oscillations during the oxidation of formic acid in perchloric acid [3].

Owing to experimental difficulties, quantitative data for oscillations of surface energy at solid electrodes are rare. Changes of surface energy may either be obtained using a piezoelectric element [26–28], or by measuring strain (i.e. the deformation of the electrode) and calculating stress from the appropriate form of Hooke's law depending on the geometry of the electrode. Specific examples of the latter class of methods are the "bending beam", the "bending plate", and the "cantilever bending" [3, 29–35]. Most methods have some drawbacks; i.e. they are technically demanding or cannot be used to monitor continuous changes of the surface energy quantitatively, because the calculation of stress from strain depends on the mechanical properties of the electrode including its support. Thus, assumptions are often used which have not been tested experimentally.

Although the piezoelectric technique is capable of detecting changes of surface energy sensitively, it is rather inappropriate for measurements at constant current density. However, improved bending beam or bending plate techniques combined with optical position detection have made possible the accurate "in situ" measurements of changes of the deformation of electrodes [3, 30, 33–38]. Using an electrode on an AT-cut quartz plate in the electrochemical Kösters-interferometer setup provides the advantages of simultaneous measurements of superficial mass and charge in addition to the deformation from which changes of specific surface energy can be calculated after experimental calibration.

In this paper, we report experiments regarding the simultaneous periodic changes of electrode potential, superficial mass, and surface energy of a platinum electrode during galvanostatic oxidation of formic acid in perchloric acid and sulphuric acid solutions.

Experimental

Methods for the measurement of surface energy

Electrochemical Koesters laser interferometry

Figure 1 shows the principle of electrochemical Koesters laser interferometry for the determination of changes of surface energy by the resulting deformation of an elastic plate. As described earlier [30, 31, 38, 39], the height ΔZ_C of the center of the plate with respect to a plane at a given radius yields changes of surface energy $\Delta\,\gamma^s$ from the appropriate form of Hooke's law

$$\Delta\gamma^s = k\Delta Z_C. \tag{1}$$

Choosing a circular AT-cut quartz plate with a thin metal layer on it in contact with the solution being the working electrode in an electrochemical cell provides the advantage to measure simultaneously surface energy, mass, and charge.

The constant k in Eq. 1 is determined completely by the mechanical properties of the quartz plate, by the type, and quality of the support at the edge of the plate. Based on the work of Janda and Stefan [40], the value $k = 15.39$ mN m^{-1} nm^{-1} was calculated [30] for a force-free support. The same value was observed in calibration experiments for a silicone glue as the support. The sensitivity is of the order of 0.1 nm with respect to ΔZ_C and mN/m with respect to $\Delta\,\gamma^s$.

The electrodes on both sides of the quartz disc were connected to an oscillator circuit. Frequencies, f, were measured with a frequency counter (Racal Dana, model 1991, or Phillips PM 6685). The changes of superficial mass $\Delta m/A$ were calculated from the changes of the frequency, Δf, using the equation [41]

$$\frac{\Delta m}{A} = K_f \Delta f \tag{2}$$

with $K_f = -4.42$ ng s cm^{-2}, A being the surface area of the platinum layer contacting the electrolyte. Thus, changes in the sensitivity level of 0.1 Hz at a fundamental frequency of 10 MHz correspond to a mass of about 0.4 ng cm^{-2}.

A low-noise battery potentiostat (Jaissle 1001 TNC) was connected to the cell for potentiodynamic and galvanostatic experiments. The electrode potential and the voltage proportional to current were digitized by a 16-bit AD/DA converter. The signal from the photodiode behind a small hole in the screen on which the interferogram was projected was fed to an impedance converter (Jaissle mV meter FET K10) with an input impedance of 10^{15} Ω and a 7 1/2 digit voltmeter (Solartron 7071). All measuring devices were controlled by a personal computer.

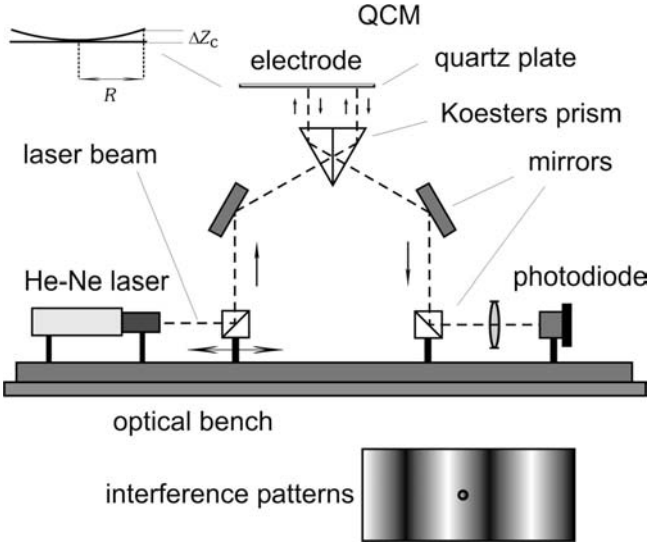

Fig. 1 The Koesters laser interferometer. R radius of the quartz plate, ΔZ_C the height of the center of the plate with respect to a plane at a given radius ("deflection")

The "bending beam" method

The changes of the surface energy $\Delta\gamma^s$ for a thin metal film on one side of a glass plate in contact with the solution were estimated from the changes of the curvature of the plate. If the thickness of the film t_f is sufficiently smaller than the thickness of the plate, $t_s >> t_f$, the change of γ^s can be obtained by an expression based on Stoney's equation [42–45]

$$\Delta\gamma^s = k_i \Delta\left(\frac{1}{R}\right), \tag{3}$$

where

$$k_i = \frac{E_s t_s^2}{6(1-\nu_s)}. \tag{4}$$

According to Stoney's theory, in Eq. 4 E_s, ν_s, and R are the Young's modulus, the Poisson's ratio and the radius of curvature of the plate, respectively. Thus,

$$\Delta\gamma^s = \frac{E_s t_s^2}{6(1-\nu_s)}\Delta\left(\frac{1}{R}\right). \tag{5}$$

The derivation of Eq. 3 implies the assumption that $\Delta\gamma^s = t_f\,\Delta\sigma_f$, where $\Delta\sigma_f$ is the change of the film stress. According to Eq. 3, for the calculation of $\Delta\gamma^s$ the changes of the reciprocal radius $\Delta(1/R)$ of curvature of the plate must be known. The values of $\Delta(1/R) = \Delta\gamma^s/k_i$ can be calculated, if the changes $\Delta\theta$ of the deflection angle θ of a laser beam mirrored by the metal layer on the plate are measured using an appropriate experimental setup as shown in Fig. 2, [46, 47].

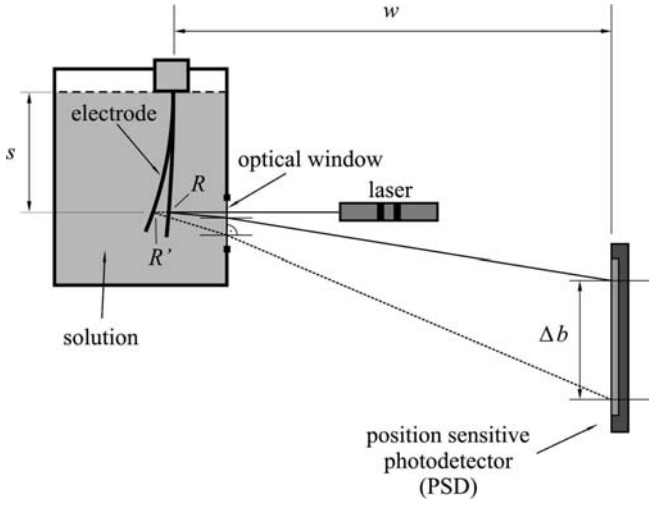

Fig. 2 Scheme of the bending beam set-up. R, R' electrode with the radius of curvature R and R'; s distance between the level of the solution in the cell and the reflection point of the laser beam on the glass plate covered by a thin platinum layer; w distance between the electrode and the position sensitive photo detector (PSD); Δb change of position of the light spot on the PSD due to the reflected beam

For the geometry shown in Fig. 2, the following approximate equation can be derived for large R and s, and small θ:

$$\Delta\left(\frac{1}{R}\right) \approx \frac{\Delta\theta}{2n_{s,i}s} \approx \frac{\Delta b}{2n_{s,i}sw}, \tag{6}$$

where s is the distance between the level of the solution in the cell (practically the lower end of the electrode holder) and the reflection point of the laser beam on the glass plate covered by a thin metal layer; w is the distance between the electrode and the position sensitive photo detector (PSD) and Δb is the change of the position of the light spot on the PSD. (Equation 6 is a good approximation only if the distance of the electrode from the optical window can be neglected compared to that of the PSD). Since the laser beam is reflected inside the solution as shown in Fig. 2, and the deflection is measured outside the cell (in the air), the refractive index $n_{s,i}$ of the solution also must be taken into account.

Consequently, from Eqs. 3 and 6 at small deflections one obtains with good approximation the relation

$$\Delta\gamma^s \approx \frac{k_i\,\Delta b}{2n_{s,i}sw}. \tag{7}$$

If the actual values of k_i (or t_s, E_s, ν_s), w, s, and $n_{s,i}$ are known, for the calculation of $\Delta\gamma^s$ only the experimental determination of Δb is necessary.

The position-sensitive detector (Hamamatsu Inc., S1300), the He–Ne laser (Melles Griot 05-LHP-151) and the electrochemical cell were assembled on an optical bench in order to avoid vibrations. The changes of output DC signals of the PSD were converted into the changes of position of the reflected beam on the PSD, that is Δb. All measuring devices were controlled by a personal computer.

Electrodes and materials

For experiments with the Koesters interferometer and the quartz frequency balance, at first thin layers of chromium and then 150-nm-thick platinum layers with the diameter $d \sim 17$ mm and the area $A \approx 2.27$ cm^2 were sputtered onto both sides of a polished and flat AT-cut quartz plate of 20-mm diameter and a thickness $d_Q = 0.167$ mm. The platinum layer on one side of the quartz disc, in contact with the electrolyte solution, served as the working electrode. The platinum layer on the back of the quartz plate was surrounded at the edge of the plate by a 3-mm wide electrically insulated gold ring serving as a mirror in the interferometer. The quartz discs were mounted to the cell by a chemically inert glue not exerting forces to the edge of the disc. The Young's moduli of the quartz are $E_x = 7.831\times10^{10}$ Pa and $E_y = 9.066\times10^{10}$ Pa in the two perpendicular principal directions, and the respective Poisson's coefficients are $\nu_{xy} = 0.277$ and $\nu_{yx} = 0.321$.

For measurements of the changes of surface energy by the "bending beam method", a glass plate with a

total length $l_s = 6.0$ cm, a width $w_s = 0.50$ cm and a thickness $t_s = 149$ μm, and a refractive index $n_g = 1.522$ at the wavelength of the He–Ne laser was used. The mechanical properties of the glass are described by the Young's modulus $E_s = 7.09 \times 10^{10}$ N m^{-2} and Poisson's ratio $\nu_s = 0.230$. After careful cleaning of the glass plate, the working electrode was prepared by sputtering or evaporating a 150-nm-thick platinum layer on a very thin layer of titanium evaporated onto one side of the plate. The geometrical area of the electrode in contact with the solution was $A = 4 \times 0.50$ cm $= 2$ cm^2.

"Millipore" quality water, p.a. sulphuric acid (Merck), p.a. perchloric acid (Merck), and guaranteed reagent grade formic acid (Aldrich) were used for the preparation of the electrolyte. The solutions were purged with oxygen-free argon (Linde 5.0) before use and an inert gas blanket was maintained throughout the electrochemical measurements.

In all the experiments a standard three-electrode arrangement was used, where a NaCl saturated calomel electrode (SSCE) was the reference electrode and a platinum plate the counter electrode. The electrode potentials E are reported versus SSCE. The experiments were carried out at constant room temperature ($T = 25.0$ °C) in air-conditioned rooms.

Refractive indices of the electrolytes were measured with an Abbé refractometer. The refractive index of the 1.0 mol dm^{-3} perchloric acid solution at 25.0 °C is $n_{s,p,1} = 1.3393$. The refractive indices of the solutions containing both perchloric acid and formic acid are $n_{s,p,2} = 1.3400$ for 1.0 mol dm^{-3} $HClO_4$ + 0.8 mol dm^{-3} HCOOH, and $n_{s,p,3} = 1.3409$ for 1.0 mol dm^{-3} $HClO_4$ + 1.6 mol dm^{-3} HCOOH, respectively. The refractive index of the 1.0 mol dm^{-3} sulfuric acid solution at 25.0°C is $n_{s,s,1} = 1.3429$. The refractive indices of solutions containing both sulfuric acid and formic acid are $n_{s,s,2} = 1.3437$ for 1.0 mol dm^{-3} H_2SO_4 + 0.8 mol dm^{-3} HCOOH, and $n_{s,s,3} = 1.3445$ for 1.0 mol dm^{-3} H_2SO_4 + 1.6 mol dm^{-3} HCOOH, respectively.

Results and discussion

Results of potentiodynamic measurements with the electrochemical Koesters interferometer at a platinum layer in a 1 mol dm^{-3} perchloric acid solution containing 0.62 mol dm^{-3} formic acid at a sweep rate of $\nu = dE/dt = 10$ mV s^{-1} (curve 1) and $\nu = dE/dt = 5$ mV s^{-1} (curve 2) are presented in Fig. 3.

Figure 3a shows the cyclic voltammograms, Fig. 3b the simultaneously detected frequency changes, and Fig. 3c the corresponding changes of the surface energy ("voltstressograms") in a relatively wide potential range.

According to the mechanistic models discussed earlier, at least three processes occur simultaneously at the electrode surface: chemisorption of the organic molecule which is formic acid in the present case, oxidation of the chemisorbed species, and oxidation of adsorbed water on the "free" sites not occupied by chemisorbed species.

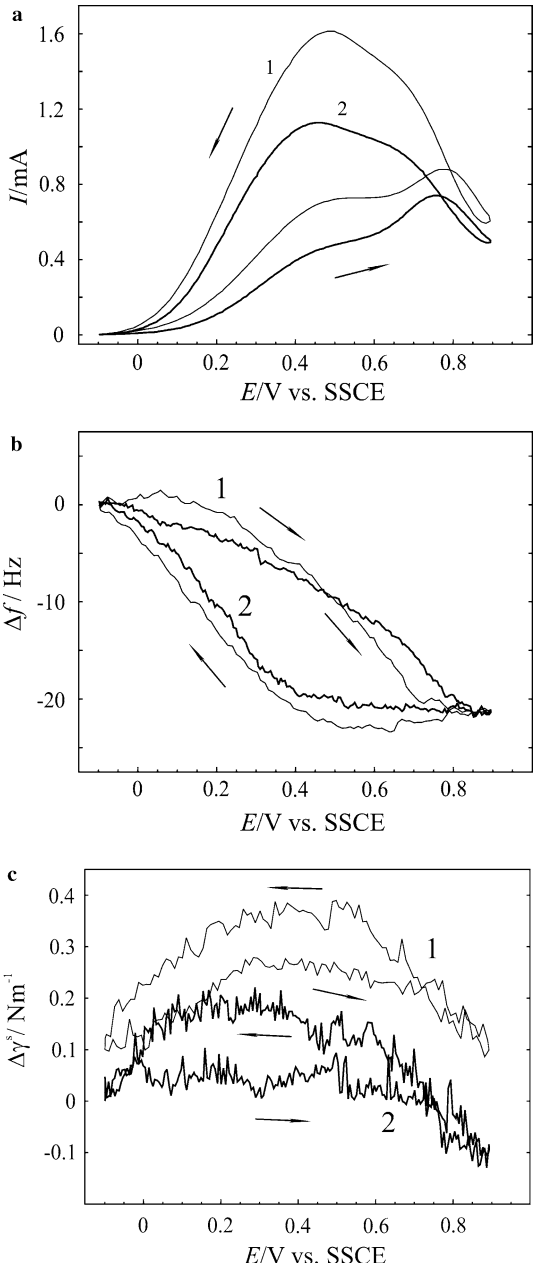

Fig. 3 **a** Cyclic voltammograms, **b** changes of the EQCM frequency Δf, and **c** changes of the radius of curvature $\Delta(1/R)$ versus electrode potential E for platinum electrodes in a solution containing $c_{HClO_4} = 1.0$ mol dm^{-3} perchloric acid and $c_{HCOOH} = 0.8$ mol dm^{-3} formic acid. Sweep rates: *1* $\nu = 10$ mV s^{-1}, *2* $\nu = 5$ mV s^{-1} (the origin of curve 1 in **c** was shifted arbitrarily)

The chemisorption involves dehydration, which causes the decrease of the potential, the rupture of bonds, possibly the splitting of the molecule, and charge transfer. The oxidation of the products of chemisorption starts only above certain potentials $E \sim 0.50$ V versus SSCE, in the present case, and the chemisorbed species is completely removed above $E \approx 0.90$ V versus SSCE. When the chemisorbed species are removed by oxidation from the surface, i.e. the number of free sites is increased, the rate of the oxidation of the chemisorbed

species yielding some definite end product which is CO_2 in the present case, increases. The voltammetric behavior of the system supports this mechanistic model. As can be seen in Fig. 3a, when the cycle is started at low potentials, the anodic current during the positive-going scan is much smaller than during the reverse scan, when the electrooxidation of formic acid takes place at the cleaned surface.

The Δf versus E and $\Delta\ \gamma^s$ versus E curves are also more or less in agreement with the above explanations. Only a small hysteresis above $E \approx 0.70$ V versus SSCE is apparent from the $\Delta\ \gamma^s$ versus E curves. The hysteresis between $E \approx -0.1$ V and 0.8 V indicates a very complex behavior in which adsorption of water [48] and oxide formation on the platinum surface at positive potentials [49] may play a significant role.

Figure 4 shows for a galvanostatic experiment a typical pattern of the simultaneous oscillations of the electrode potential, the surface energy $\Delta\ \gamma^s$, and the frequency change of the EQCM determined with the electrochemical Koesters interferometer setup. A constant current $I = 0.35$ mA was applied to the electrode immersed in a $c_{H_2SO_4} = 0.5$ mol dm^{-3} sulfuric acid solution containing 0.9 mol dm^{-3} formic acid. Oscillations start after an induction period. In general, under the same conditions of current density and composition of the solution the oscillation experiment can be repeated several times. The induction period is most likely due to the slow accumulation of adsorbed species poisoning the electrode [48]. According to curves a and c, the rapid decrease of the potential apparently is accompanied by a fast increase of the superficial mass, i.e. by a fast decrease of the frequency. As the potential increases again, the frequency of the EQCM also increases. The changes of γ^s also follow the changes of the electrode potential. As the potential increases, the specific surface energy decreases. The rapid decrease of the potential is accompanied by a rapid increase of γ^s.

Typical pattern of the simultaneous oscillations of the electrode potential and the reciprocal radius of curvature of the electrode ($\Delta(1/R) = \Delta\gamma^s/k_i$) determined with the bending beam method are shown in Fig. 5.

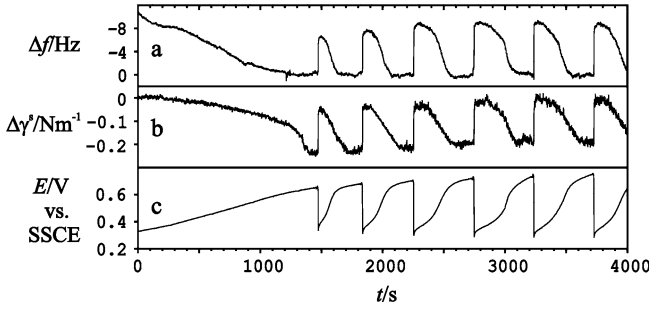

Fig. 4 Typical oscillation patterns for the galvanostatic oxidation (current density: $i = 0.15$ mA cm^{-2}) of formic acid at a platinum electrode in a solution containing $c_{H_2SO_4} = 0.5$ mol dm^{-3} sulphuric acid and $c_{HCOOH} = 0.9$ mol dm^{-3}: **a** changes of frequency Δf of the EQCM (10 MHz, AT quartz), **b** changes of surface energy $\Delta\gamma^s$, and **c** electrode potential E as a function of time t

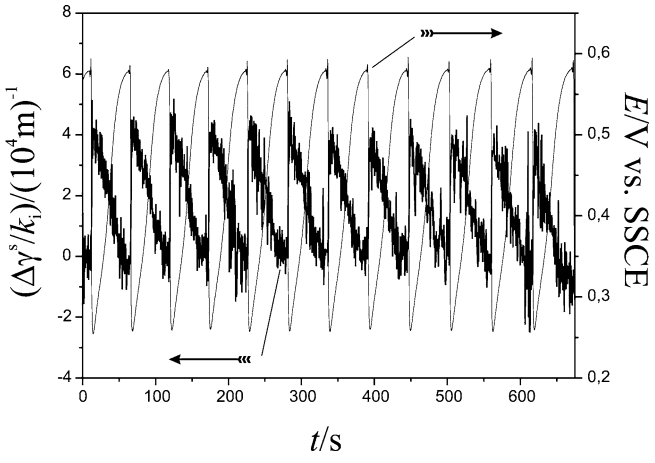

Fig. 5 Typical oscillation patterns for the galvanostatic oxidation (current density: $i = 0.2$ mA cm^{-2}) of formic acid at platinum in a solution containing $c_{HClO_4} = 1.0$ mol dm^{-3} perchloric acid and $c_{HCOOH} = 1.6$ mol dm^{-3} formic acid: oscillations **a** of the electrode potential E and **b** of the reciprocal radius of curvature $\Delta\ (1/R) = \Delta\ \gamma^s/k_i$

It should be noted here that although Stoney's equation has been—and still is—extensively used to evaluate the stress acting in a coating deposited on a thick substrate, several modifications to the original equation has been proposed in the literature [50, 51], but the more complex equations reduce to Eq. 3 in the special case of a very thin film on a substrate. However, the values of k_i differ in the different theories. Stoney's original formula $k_1 = E_s\ t_s^2/6\ (1 - \nu_s)$ with the material constants of the bending beam used in the present experiments yields $k_1 \approx 340.6$ Nm^{-1}, and the formula $k_2 = E_s t_s^2/12\ (1 - \nu_s)$ proposed by Chou [50] yields $k_2 \approx 170.3$ Nm^{-1}. Since the correct value of k_i in Eqs. 3 and 6 thus is uncertain, only the values of $\Delta\ (1/R) = \Delta\ \gamma^s/k_i$ are given in the figures showing the results of bending beam experiments.

The curves in Fig. 5 were obtained with a constant current $I = 0.4$ mA for the platinum electrode in a 1.0 mol dm^{-3} perchloric acid solution containing 1.6 mol dm^{-3} formic acid. Although the deflection of the electrode varies with the periodicity of the potential jumping from its minimum to its maximum in correspondence with the periodic potential change, an increase of its mean value can be observed. Typically, the increase is faster at the beginning of the experiments, and decays continuously afterwards, as shown in Fig. 6 in which the starting period of two experiments carried out in perchloric acid ($c_{HClO_4} = 1$ mol dm^{-3}) and sulfuric acid ($c_{H_2SO_4} = 1$ mol dm^{-3}) solutions containing formic acid ($c_{HCOOH} = 0.8$ mol dm^{-3}) are presented.

According to Fig. 6, the shift of the surface energy at the beginning of the experiment is more pronounced for perchloric acid than for sulfuric acid as the supporting electrolyte.

However, the origin of the continuous shift of the mean value of the deflection is not quite clear. Previously Kertész et al. [23] reported a similar phenomenon observed at PBD experiments, and they attributed it to the

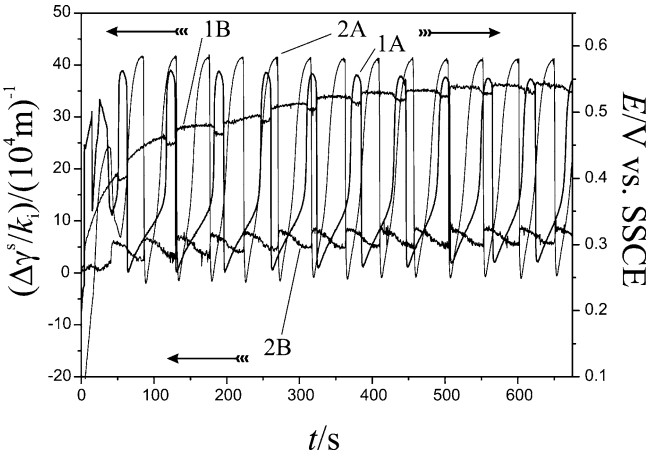

Fig. 6 Induction period and beginning of oscillations. (1A, 2A) electrode potential E; (1B, 2B) changes of the reciprocal radius of curvature $\Delta(1/R) = \Delta\gamma^s/k_i$ of the bending beam. (1A, 1B): solution containing $c_{HClO_4} = 1.0\,mol\,dm^{-3}$ perchloric acid and $c_{HCOOH} = 0.8$ mol dm^{-3} formic acid; (2A, 2B): solution containing $c_{H_2SO_4} = 1.0\,mol\,dm^{-3}$ sulfuric acid and $c_{HCOOH} = 0.8$ mol dm^{-3} formic acid. Current density $i = 0.2$ mA cm^{-2}

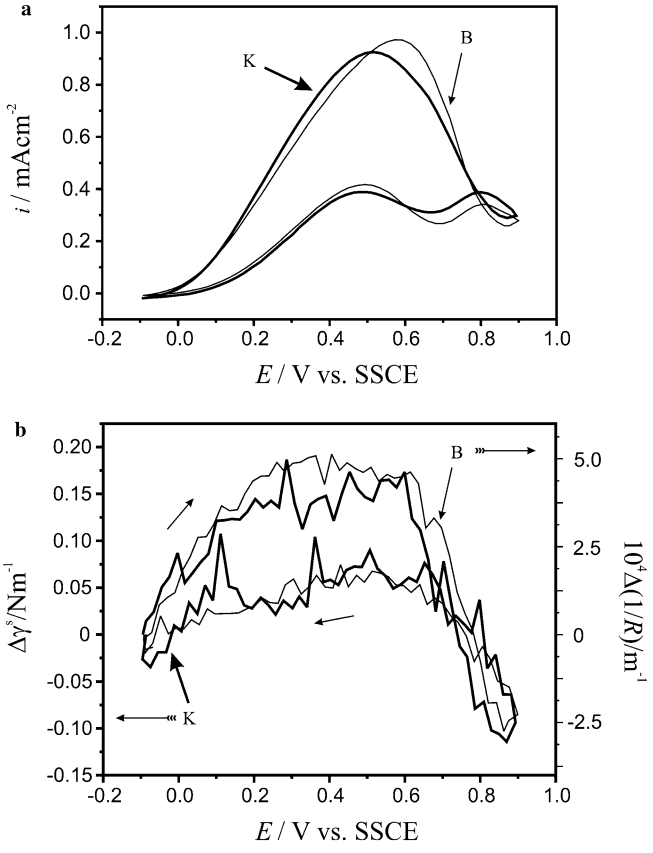

Fig. 7 **a** Cyclic voltammograms; **b** changes of specific surface energy $\Delta\gamma^s$ and changes of the reciprocal radius of curvature $\Delta(1/R) = \Delta\gamma^s/k_i$ vs. electrode potential E obtained with platinum in contact with solutions containing $c_{H_2SO_4} = 1.0\,mol\,dm^{-3}$ sulfuric acid and $c_{HCOOH} = 0.8$ mol dm^3 formic acid. Sweep rate: $v = 20$ mV/s. *K* from experiments with the Kösters laser interferometer, *B* from experiments with the bending beam

continuous build up of the concentration gradient occurring near the electrode surface under conditions of constant current and unstirred solution. This interpretation cannot hold in the present case, since the laser beam is reflected from the reverse side of the platinum layer, which is not in contact with the solution. In principle, the deflection of the electrode may have two origins: the changes of the surface stress due to adsorption, and thermal effects. Since the difference of the thermal expansion coefficients of the substrate and that of the thin platinum layer is very small, effects originating from the systematic change of the temperature close to the electrode may be also small. In addition, the direction of the observed change of the deflection would indicate an improbable lowering of the temperature at the beginning of the experiments. More probably, the slow changes of the mean value of the deflection are therefore related to slow changes of the structure of the electrode surface and to slow relaxation processes inside the metal film. On the other hand, effects of Cl^- ions formed by the (electro)reduction of ClO_4^- ions on platinum cannot be excluded [52–57]. Further experiments are necessary to clarify this issue.

As mentioned earlier, there are conflicting views regarding the calculation of k_i in Eq. 3. However, since the laser interferometer was calibrated by an independent method [30], a comparison of the results of Koesters laser interferometry and the bending beam method will yield an estimate for the "effective" value of k_i.

In Fig. 7 results of experiments with the electrochemical bending beam setup and with the Koesters laser interferometer are compared. Both setups yield practically identical cyclic voltammograms for the sputtered platinum layers in contact with mixtures of sulphuric acid and formic acid with $c_{H_2SO_4} = 1$ mol dm^{-3} and $c_{HCOOH} = 0.8$ mol dm^{-3}, respectively, at a sweep rate of $v = 20$ mV/s. On the other hand, the simultaneously recorded $\Delta\gamma^s$ vs. E curves from the interferometer experiments and the $\Delta(1/R)$ versus E curves measured by the bending beam method have very similar shapes. The ratios of the corresponding $\Delta\gamma^s$ and $\Delta(1/R)$ values calculated point by point as a function of the electrode potentials are plotted in Fig. 8 yielding a mean value $k_i \approx 300$ N. The relatively large scatter of the data is due to external mechanical noise.

The average value is about 12% larger than the value $k_1 \approx 340.6$ N, calculated from Stoney's equation with the material constants of the glass substrate, but far from the value calculated by Chu's equation. Further work regarding the calibration of the bending beam technique by an independent method is in progress.

Conclusions

The Koesters laser interferometer and the bending beam are equivalent tools to measure and monitor continuously changes of the surface energy of a solid electrode. Based on the calibration of the Koesters interferometer,

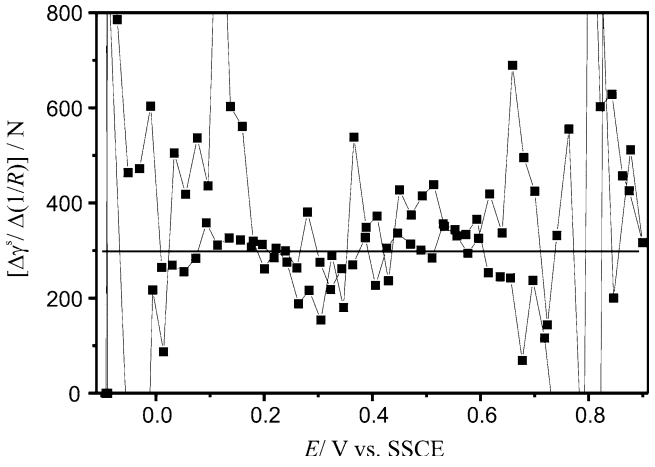

Fig. 8 The ratio of $\Delta\gamma^s$ measured by laser interferometry and $\Delta(1/R)=\Delta\gamma^s/k_i$ measured with the bending beam from experiments shown in Fig. 7. The average value of k_i for optimal agreement of surface energy is $k_i \approx 300$ N

the constant $k_i \approx 300$ N relating the change of the curvature of the bending beam to specific surface energy was obtained which within the limits of experimental accuracy is close to the value $k_1 \approx 340.6$ N calculated from Stoney's equation, but far from the value obtained from Chu's equation.

The results of electrochemical Koester laser interferometry furnished experimental evidence for simultaneous periodical changes of the surface stress, surface mass, and electrode potential in the course of galvanostatic oxidation of formic acid on platinum. The slow changes of the mean value of the deflection is probably related to slow changes of the structure of the electrode surface and to slow relaxation processes inside the metal film, but effects of Cl^- ions formed by the reduction of ClO^-_4 ions on platinum cannot be excluded.

Acknowledgements Financial support by the National Scientific Research Fund OTKA T037588, M042115, Alexander von Humboldt Stiftung, and the Japan Society for the Promotion of Science (JSPS) is gratefully acknowledged.

References

1. Wojtowitz J (1972) Oscillatory behaviour in electrochemical systems. In: Bockris JO, Conway BE (eds) Modern aspects of electrochemistry, vol 8. Plenum, New York
2. Franck UF (1974) Faraday Symp Chem Soc 9:137
3. Láng GG, Ueno K, Ujvári M, Seo M (2000) J Phys Chem B 104:2785
4. Okamoto H, Tanaka N, Naito M (1998) J Phys Chem A 102:7343
5. Okamoto H, Tanaka N, Naito M (1998) J Phys Chem A 102:7353
6. Cui H, Chen S, Zhao S, Wang C (2001) J Serb Chem Soc 66:881
7. Langa S, Carstensen J, Tiginyanu IM, Christophersen M, Foll H (2001) Electrochem Solid State Lett 4:G50
8. Li ZL, Niu ZJ, Wu TH, Nie HD, Xiao XM (2003) Electrochem Commun 5:297
9. Darowicki K, Krakowiak A, Zielinski A (2003) Russ J Electrochem 39:935
10. Chen A, Miller B (2004) J Phys Chem B 108:2245
11. Krischer K (2003) Nonlinear dynamics in electrochemical systems. In: Alkire RC, Kolb DM (eds) Advances in electrochemical science and engineering, vol 8. Wiley-VCH, Weinheim, pp 89–208
12. Horányi G, Inzelt G, Szetey E (1978) Acta Chim Acad Sci Hung 97:299
13. Inzelt G, Kertész V (1995) Electrochim Acta 40:221
14. Koper M, Hachkar M, Beden BJ (1996) Chem Soc Farad Trans 92:3975
15. Albahadily FN, Schell M (1991) J Electroanal Chem 308:151
16. Naito M, Okamoto H, Tanaka N (2000) Phys Chem Chem Phys 2:1193
17. Albahadily FN, Schell M (1991) J Electroanal Chem 308:151
18. Strasser P, Eiswirth M, Ertl G (1997) J Chem Phys 107:991
19. Okamoto H, Tanaka N, Naito M (1996) Chem Phys Lett 248:289
20. Naito M, Okamoto H, Tanaka N (2000) Phys Chem Chem Phys 2:1193
21. Horányi G, Inzelt G (1978) J Electroanal Chem 87:423
22. Conway BE, Novak DM (1977) J Phys Chem 81:1459
23. Kertész V, Inzelt G, Barbero C, Kötz R, Haas O (1995) J Electroanal Chem 392:91
24. Inzelt G, Kertész V, Láng G (1993) J Phys Chem 97:6104
25. Trasatti S, Parsons R (1986) Pure Appl Chem 58:437
26. Ya A (1976) Gokhshtein, in "Surface Tension of Solids and Adsorption". Nauka, Moscow
27. Seo M, Makino T, Sato N (1986) J Electrochem Soc 133:1138
28. Seo M, Jiang XC, Sato N (1987) J Electrochem Soc 134:3094
29. Morcos I (1978) "Specialist Periodical Reports Electrochemistry", vol 6. In: Thirsk HR (ed) The Chemical Society, Burlington House, London,
30. Jaeckel L, Láng G, Heusler KE (1994) Electrochim Acta 39:1081
31. Láng G, Heusler KE (1995) J Electroanal Chem 391:169
32. Ibach H (1997) Surface Sci Rep 29:193
33. Heusler KE, Láng G (1997) Electrochim Acta 42:747
34. Láng GG, Seo M (2000) J Electroanal Chem 490:98
35. Haiss W (2001) Rep Prog Phys 64:591
36. Ueno K, Seo M (1999) J Electrochem Soc 146:1496
37. Heusler KE, Láng G (1997) Electrochim Acta 42:747
38. Láng G, Heusler KE (1997) J Chem Soc Farad Trans 93:583
39. Heusler KE, Lang G (1995) Elektrokhimiya 31:826
40. Janda M, Stefan O (1984) Thin Solid Films 112:127
41. Sauerbrey G (1959) Z Phys 155:206
42. Stoney GG (1909) Proc R Soc Lond A 32:172
43. Suhir E (1988) J Appl Mech 55:143
44. Moulard G, Contoux G, Gardet G, Motyl G, Courbon M (1997) Surf Coat Technol 97:206
45. Moulard G, Contoux G, Motyl G, Gardet G, Courbon M (1998) J Vac Sci Technol A 16:736
46. Láng GG, Ueno K, Ujvári M, Seo M (2000) J Phys Chem B 104:2785
47. Láng GG, Seo M (2000) J Electroanal Chem 490:98
48. Okamoto H, Tanaka H (1992) Electrochim Acta 37:37
49. Beck TR, Lin K-F (1979) J Electrochem Soc 126:252
50. Chu SNG (1998) J Electrochem Soc 145:3621
51. Klein CA (2000) J Appl Phys 88:5487
52. Ya Vasina S, Petrii OA (1970) Elektrokhimiya 6:242
53. Horányi G, Vértes G (1975) J Electroanal Chem 64:252
54. Bakos I, Horányi G (1992) J Electroanal Chem 332:147
55. Horányi G, Bakos I (1992) React Kinet Catal Lett 46:139
56. Horányi G, Bakos I (1992) J Electroanal Chem 331:727
57. Láng GG, Horányi G (2003) J Electroanal Chem 552:197